

Damage and Recovery of Aluminum for Low-Energy Electron Irradiations*

H. M. SIMPSON† AND R. L. CHAPLIN

Department of Physics, Clemson University, Clemson, South Carolina 29631

(Received 10 March 1969)

Damage rates for samples of high-purity aluminum have been measured as a function of the electron irradiation energy from 0.16–0.40 MeV. A detailed analysis of the data is presented and the results indicate that the threshold energy for an atomic displacement in aluminum is 16 eV. Experimental values of the fractional amount of stage-I recovery show that the percentage of stage I is not a simple function of the irradiation energy. The observed energy dependence is explained in terms of the production of subthreshold damage events.

I. INTRODUCTION

PREVIOUS studies^{1–3} have been made of the energy dependence of the rate of damage production for high-purity aluminum. This paper extends those results to lower irradiation energies. The data are corrected for electron straggling,⁴ for electron energy degradation due to sample thickness,⁵ and for an initial energy distribution of the irradiating electron beam. Prior results that were based on damage-rate studies have indicated that subthreshold damage⁶ is apparently absent for aluminum.^{1,7} Damage-rate results reported in this work support that conclusion, however, the energy dependence of stage-I recovery provides a more precise analysis of the data and indicates that a small amount of subthreshold damage does occur for this metal.

II. EXPERIMENTAL

Some of the parameters that determine the precision of experimental results for electron-irradiation studies become most important for low values of the irradiation energy. For this reason, measurements have been made⁸ of the energy distribution of the energetic electron beam from our Van de Graaff accelerator. It was found that the average energy of the primary electrons is defined to within ± 4 keV. The energy distribution of the electrons can be approximated by a Gaussian distribution with a 15-keV half-width for the 0.1–0.4-MeV energy range. When the electrons irradiate a sample, the total electron flux is measured by an Elcor current integrator (Model

A 309), and the estimated error of this flux value does not exceed $\pm 5\%$.

The methods of preparing and mounting samples have been described elsewhere.⁹ Results for this report were obtained from one high-purity aluminum sample that had a thickness of 0.005 cm and an irradiated length of 25 cm. During irradiation, the temperature of the sample did not exceed 10°K. Potentiometric measurements of the sample were performed when the sample temperature was 4.2°K. Because the sample had a large ratio of length to cross-sectional area, changes of electrical resistivity of $4 \times 10^{-13} \Omega \text{ cm}$ were readily evaluated. The reliability of the data is indicated by the linearity of the experimental results of the changes of resistivity versus irradiation flux that are shown in Fig. 1. Data for any one irradiation energy determine a straight line whose slope corresponds to the damage-rate value.

III. DAMAGE RATES

Experimental results of damage rates are presented in Fig. 2 where the open circles give the measured values of damage rate in terms of an average electron irradiation energy \bar{E} . This average energy was calculated¹ from

$$\bar{E} = E_i - at_0/2, \quad (1)$$

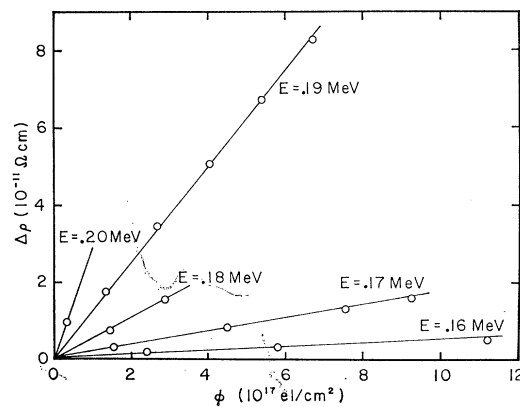


FIG. 1. Open circles show experimental results of the change of electrical resistivity as a function of the dose of electron irradiation for the designated irradiation energies.

* R. L. Chaplin and H. M. Simpson, Phys. Rev. **163**, 587 (1967).

* Work supported by the U. S. Atomic Energy Commission.
† Present address: Department of Physics, University of Utah, Salt Lake City, Utah.

¹ H. H. Neely and W. Bauer, Phys. Rev. **149**, 535 (1966).

² G. W. Iseler, H. I. Dawson, A. S. Mehner, and J. W. Kauffman, Phys. Rev. **146**, 468 (1966).

³ P. G. Lucasson and R. M. Walker, Phys. Rev. **127**, 485 (1962).

⁴ A. Sosin and W. Bauer, in *Studies in Radiation Effects*, edited by G. J. Dienes (Gordon and Breach, Science Publishers, Inc., New York, 1968).

⁵ M. J. Berger and M. S. Stephen, National Academy of Science National Research Council, Nuclear Science Series Report No. 39, 205–208, 1964 (unpublished).

⁶ W. Bauer and A. Sosin, J. Appl. Phys. **35**, 703 (1964).

⁷ W. Bauer, in *Lattice Defects and Their Interactions*, edited by R. R. Hasiguti (Gordon and Breach, Science Publishers, Inc., New York, 1966).

⁸ R. E. Longshore, Ph.D. dissertation, Clemson University, 1968 (unpublished).

where E_i is the incident electron energy, α is the electron energy loss per unit distance,⁵ and t_0 is the thickness of the foil. When a correction is made for electron straggling,⁴ the experimental data shift from the open-circle positions to lower damage-rate values indicated by the solid circles. Although this correction is relatively large and unreliable, both sets of data (open and solid circles) give practically the same energy dependence of the damage rate. Also, the correction for electron straggling does not affect the evaluation of the threshold energy T_d . No correction has been applied to the data for the electrical size effect⁴ which should be negligible for these 50- μm foils.¹⁰

To compare the experimental values of damage rate to theoretical results, it is assumed that the aforementioned corrections to the data are valid, the incident irradiating electrons are monoenergetic, and no multiple atomic displacements occur for these irradiation energies. Theoretical calculations of damage rates are performed by using

$$\frac{\Delta\rho}{\Delta\phi} = \rho_F \int_0^{T_m(E)} P(T) \frac{d\sigma}{dT} dT, \quad (2)$$

where ρ_F is the resistivity of a unit concentration of Frenkel pairs, $T_m(E)$ is the maximum atomic recoil energy for the irradiation energy E , $P(T)$ is the probability of atomic displacement, and $d\sigma/dT$ is the differential cross section for elastic collisions between electrons and stationary nuclei.¹¹ Equation (2) was used to calculate the curves that are shown in Fig. 2 for specific $P(T)$ functions and ρ_F values as tabulated on the figure. When the irradiation energy is greater than 0.2 MeV, curves a and c provide the best approximation of the energy dependence of the damage rate. Neely and Bauer¹ have also concluded that the parameters which describe the above c curve provide good agreement with their experimental data.

Because Fig. 2 indicates that theory does not fit the data for the low-energy region, let us consider the following experimental facts: (i) When the electron irradiation energy is only slightly above the threshold-energy region, most of the defects are produced near one surface of the sample; thus, the average electron irradiation energy cannot be evaluated by using half the foil thickness as expressed in Eq. (1). (ii) Measurements of damage rate for the threshold-energy region cannot indicate a well-defined threshold-energy value because of the energy distribution of the irradiating electron beam. In other words, it is not valid to approximate the energy distribution of the irradiating electrons by an average irradiation energy. To note the influence of these two effects, the following equations modify the theoretical treatment when the probability for an atomic displacement is the multiple step function; i.e., curve a of Fig. 2. Let us limit the maximum atomic

¹⁰ F. Dworschak, H. Schuster, H. Wollenberger, and J. Wurm, *Phys. Status Solidi* **21**, 741 (1967).

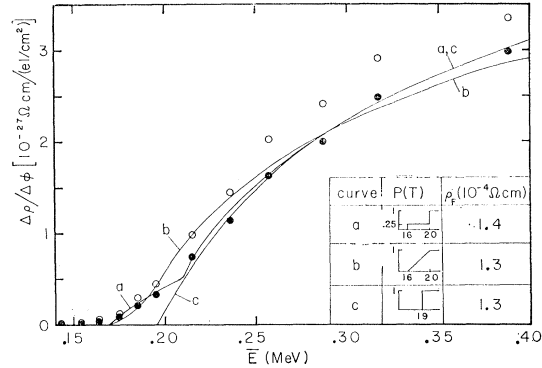


FIG. 2. Open circles indicate measured values of damage rates and solid circles give damage-rate values which are corrected for electron straggling. The solid lines were determined by theoretical calculations of damage rate in accordance to the quantities indicated on the figure.

recoil energy to values that are less than 20 eV, and let the cross section for an atomic displacement¹¹ be

$$\sigma_d = \frac{0.2495}{4} \frac{Z^2}{\beta^4 \gamma^4} \left[\frac{T_m(E)}{T_d} - 1 \right] b, \quad (3)$$

where Z is the atomic number, $\beta = V/c$, $\gamma = (1 - \beta^2)^{-1/2}$, and V is the velocity of the electron. The theoretical cross section expressed by Eq. (3) is now used to determine the effect of the different corrections. One can compensate for the electron energy degradation caused by the sample thickness, by averaging¹² the cross section over the foil thickness τ_0 . This correction is applied to the cross section by using

$$\bar{\sigma}_d(E_i, \tau_0) = \frac{1}{\tau_0} \int_0^{\tau_0} \sigma_d[E(\tau)] d\tau, \quad (4)$$

where the electron energy for a thickness τ , $E(\tau)$, is determined from the known electron-energy-loss rates. By assuming that the electron paths are straight lines, Eq. (4) is readily integrated numerically. Correcting the cross section for a nonmonoenergetic electron beam is done by assuming that the electron energy distribution is described by a Gaussian function, $F(E, E_i)$, which is centered about the primary irradiation energy E_i . Thus,

$$\sigma_d(E_i) = \int_{E_0}^{\infty} F(E, E_i) \sigma_d(E) dE, \quad (5)$$

where E_0 is the electron irradiation energy for $T_m = T_d$. To show the effect of these corrections, the variation of the cross sections for aluminum is plotted versus the irradiation energy in Fig. 3. Curve a shows the uncorrected theoretical cross section as expressed by Eq. (3). By compensating for the electron energy loss as de-

¹¹ F. Seitz and J. S. Koehler, in *Solid State Physics*, edited by F. Seitz and D. Turnbull (Academic Press Inc., New York, 1956), Vol. II, pp. 330-331.

¹² W. E. Gettys, *Phys. Rev.* **146**, 480 (1966).

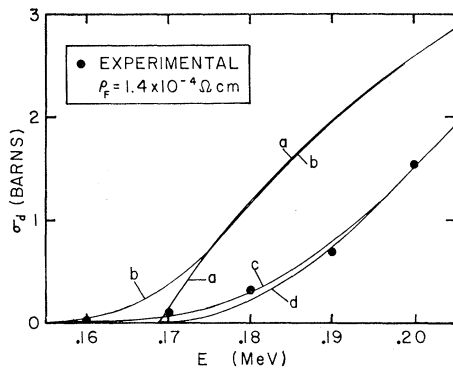


FIG. 3. Experimental data are plotted in terms of the irradiation energy and the cross section for an atomic displacement as given by curve (a) is corrected for electron energy loss to give (d) and is corrected for the energy distribution of the irradiating electrons to give (b). Applying both corrections to (a) gives (c).

terminated from Eq. (4), curve d is obtained. It is evident that this modification produces a "tailing off" of the cross section for the low energies so that the curve approaches the experimentally observed results shown by the solid points. When the irradiation energy is well above the threshold-energy region, then

$$\bar{\sigma}_d(E, \tau_0) \rightarrow \sigma_d(\bar{E}), \quad (6)$$

and this correction is readily given by Eq. (1). The influence of the electron distribution function, i.e., the application of Eq. (5), is represented by curve b on Fig. 3. This curve shows that the beam distribution causes an apparent shift of data to lower-energy values. When the theoretical calculation of the cross section for atomic displacements is corrected for both energy loss and energy distribution of the electron beam, curve c is obtained and this result shows very good agreement with the plotted experimental values.

IV. ENERGY DEPENDENCE OF STAGE-I RECOVERY

Even if the experimental values of the total damage rate for the 0.16- and 0.17-MeV irradiation energy were in error by 50%, the results of the preceding analysis are still valid because these quantities have such a small magnitude. Therefore, a more precise analysis of the experimental data is desired. The following gives an alternative method for examining the energy depend-

TABLE I. Energy dependence of stage-I recovery.

Irradiation energy (MeV)	Measured values of stage-I recovery (%)	Corrected values of stage-I recovery (%)
0.16	65 ± 5	100
0.17	89 ± 2	98
0.19	92 ± 0.5	94
0.22	93 ± 0.5	93
0.30	88.2 ± 0.3	88.2
0.40	84.3 ± 0.2	84.3

ence of the damage which is based on the fraction of the total damage that anneals during stage I.⁹

The experimentally determined values for the percentage recovery of stage I for each irradiation energy are given in the second column of Table I. Note how the amount of stage-I recovery has a consistent decrease for irradiation energies above and below 0.22 MeV. This energy-dependent variation has a simple explanation if one assumes that there are two distinct mechanisms for damage production. Let the total damage rate $(\Delta\rho/\Delta\phi)_T$ consist of (i) an intrinsic rate for damage production $(\Delta\rho/\Delta\phi)_i$, which has an energy dependence that is explained in the preceding section, and (ii) a subthreshold¹³ damage rate $(\Delta\rho/\Delta\phi)_0$ that is energy-independent. (This subthreshold damage may be associated with impurity atoms⁶ and does not anneal during Stage I.) Thus,

$$\left(\frac{\Delta\rho}{\Delta\phi}\right)_T = \left(\frac{\Delta\rho}{\Delta\phi}\right)_i + \left(\frac{\Delta\rho}{\Delta\phi}\right)_0. \quad (7)$$

An evaluation of $(\Delta\rho/\Delta\phi)_0$ is obtained by assuming that for the low irradiation energy of 0.16 MeV, the intrinsic damage consists of only close pairs of Frenkel defects which recover within stage I. (The justification for this assumption is based on the extrapolation of the energy dependence of stage I from the highest-irradiation-energy region.) The total damage rate for the 0.16-MeV irradiation is therefore distributed in accordance to

$$\left(\frac{\Delta\rho}{\Delta\phi}\right)_i = 0.65 \left(\frac{\Delta\rho}{\Delta\phi}\right)_T,$$

and

$$\left(\frac{\Delta\rho}{\Delta\phi}\right)_0 = 0.35 \left(\frac{\Delta\rho}{\Delta\phi}\right)_T,$$

where the numerical values are from Table I. Because the subthreshold damage is energy-independent, the magnitude of $(\Delta\rho/\Delta\phi)_0$ can be subtracted from the measured damage rates of other irradiation energies. This procedure then gives corrected magnitudes for the intrinsic damage rate. To show the effect of this correction, computed values for the fractional amount of stage-I recovery are presented in the third column of Table I. These results show that (i) this correction is significant for the lowest irradiation energies only and (ii) stage-I recovery can be interpreted as a progressively decreasing quantity for increasing values of the irradiation energy.

V. CONCLUSION

For irradiation energies greater than 0.20 MeV, the results of this study are in good agreement with the work of Neely and Bauer¹ where it was concluded that an effective threshold energy of 19 eV and a simple step function provide an accurate description of damage production in aluminum. An investigation of damage

¹³ W. Bauer and A. Sosin, *J. Appl. Phys.*, **37**, 1780 (1966).

rates for irradiation energies from 0.15 to 2.1 MeV has been performed by Iseler *et al.*² The analysis of those data dealt with the entire energy range so that the features of multiple-atomic-defect production were emphasized. This paper shows that for irradiation energies less than 0.20 MeV the theoretical and experimental damage rates have the best agreement when the probability of atomic displacement is a multiple step function (see curve a of Fig. 2). Uncertainties are present in the analysis because the magnitudes of the corrections are of the order of the experimental values. It is shown that each correction introduces an effect that prevents a well-defined intersection between the damage-rate curve and the abscissa. It is evident from these results that high-purity aluminum does not have an appreciable amount of subthreshold damage.

It is generally accepted¹⁴ that the electron irradiation of a metal produces simple point defects of interstitials and vacancies. Defects which recover during stage I are

¹⁴ J. W. Corbett, in *Solid State Physics*, edited by F. Seitz and D. Turnbull (Academic Press Inc., New York, 1966).

caused by the annihilation of interstitials which are either bound to vacancies (these reactions obey first-order kinetics) or migrate through the lattice (diffusion-limited reaction). Trapping is a mechanism which prevents the complete recombination of interstitials and vacancies during stage I. Because trapping is a process that depends on the distance that an interstitial is separated from its initial lattice site, one deduces that the fraction of the damage which does not anneal during stage I should increase monotonically with the irradiation energy.⁹ In order to obtain the desired energy dependence for the stage-I recovery of aluminum, the total induced damage has been resolved into subthreshold and intrinsic components, and the subthreshold damage is assumed to be independent of the irradiation energy. The calculations based on these assumptions give results which account for the observed energy dependence of stage I for aluminum. This interpretation of the data is consistent with the known facts that the amount of subthreshold damage is appreciable for copper¹³ but small for aluminum.¹

Coherent Neutron Scattering by Cobalt with Nuclear Polarization*

Y. ITO† AND C. G. SHULL

Massachusetts Institute of Technology, Cambridge, Massachusetts 02139

(Received 10 March 1969)

The polarized-neutron diffraction technique has been used to determine the modification of coherent scattering with nuclear polarization in cobalt. This was studied in two Bragg reflections, (220) and (140), from a crystal of hexagonal cobalt at temperatures as low as 2.23°K, with nuclear polarization being developed by hyperfine field interaction in the ferromagnetic element. From these observations, the spin-state scattering amplitudes b_+ and b_- , corresponding to neutron-nucleus compound states of spin $I+\frac{1}{2}$ and $I-\frac{1}{2}$, respectively, have been determined as $(-0.380 \pm 0.054) \times 10^{-12}$ and $(+1.060 \pm 0.070) \times 10^{-12}$ cm. These values are found to be consistent with the coherent scattering amplitude as obtained in unpolarized-neutron-unpolarized-nucleus studies, and with the known neutron resonance level structure in cobalt.

I. INTRODUCTION

THE scattering of thermal neutrons by nuclei of spin I is described in terms of the two spin-state amplitudes b_+ and b_- , which are associated with the total spin states $I+\frac{1}{2}$ and $I-\frac{1}{2}$ of the compound neutron-nucleus system, respectively. These spin-dependent scattering amplitudes provide useful information relative to the energy levels of the compound nucleus in the vicinity of thermal energy, and in a practical sense knowledge of them is significant, since they determine the coherent and incoherent scattering to be found by an assembly of nuclei in a crystal.

If the scattering nuclei are unpolarized, as is usually the case at normal temperature, it is convenient to introduce combinations of the spin-state amplitudes into the coherent and incoherent scattering amplitudes b_c and b_i as follows:

$$b_c = \frac{I+1}{2I+1} b_+ + \frac{I}{2I+1} b_-, \quad (1)$$

$$b_i = \frac{2}{2I+1} (b_+ - b_-). \quad (2)$$

These quantities are used extensively in neutron-diffraction investigations, since they describe the nuclear-scattering contribution to the coherent Bragg intensity and the incoherent, spin disorder scattering from a crystal. Values for b_c , both in magnitude and absolute sign, have been determined by experiment for

* Research supported by the Division of Research, U. S. Atomic Energy Commission. It is based on a thesis submitted by the senior author to the Department of Physics at the Massachusetts Institute of Technology in partial fulfillment of the requirements for the degree of Doctor of Philosophy.

† Present address: Ames Laboratory, Iowa State University, Ames, Iowa 50010.